Polymer 49 (2008) 5013–5022

Contents lists available at ScienceDirect

Polymer

journal homepage: www.elsevier.com/locate/polymer

The study of water behaviour in regenerated cellulosic fibres by low-resolution proton NMR

Roger N. Ibbett [a,*], K. Christian Schuster [b,c], Mario Fasching [d]

[a] Christian Doppler Laboratory for Textile and Fibre Chemistry in Cellulosics, School of Materials, University of Manchester, Manchester M601QD, UK
[b] Lenzing AG, 4860 Lenzing, Austria
[c] Christian Doppler Laboratory for Textile and Fibre Chemistry in Cellulosics, Höchsterstraße 35, 6850 Dornbirn, Austria
[d] K+, Kompetenzzentrum Holz GmbH, St.-Peter-Strasse 25, 4021 Linz, Austria

ARTICLE INFO

Article history:
Received 30 July 2008
Accepted 22 August 2008
Available online 11 September 2008

Keywords:
Cellulose
NMR
Water

ABSTRACT

Regenerated cellulosic fibres and comparative materials were studied in the hydrated state by low-resolution proton NMR. Experiments at variable pH and temperatures have shown that the shortened T_2 relaxation times of water within fully swollen cellulosic fibres are dominated by proton exchange with accessible cellulose hydroxyl groups. Proton exchange is accelerated by both acid and base catalysis, with relaxation data used to estimate rate constants for acid, base and neutral mechanisms. Complementary deuterium exchange measurements suggest that accessible cellulose regions below the immediate water interface may not contribute effectively to the proton exchange relaxation mechanism, with two-site relaxation models sensitive only to the direct pore surface area. Differences between surface-relaxing water and deuterium-exchanging water can therefore be used to determine an apparent depth of the accessible cellulose, which is greater for viscose and modal compared to lyocell. However, from relaxation data lyocell has a higher pore surface area. This work also confirmed that water interacting with accessible cellulose experiences motional restriction, allowing an intra-molecular dipolar contribution to relaxation. However, in the fully swollen state water molecules are diffusing rapidly between all internal fibre environments and there is no evidence of specific binding.

1. Introduction

Regenerated cellulosic fibres are a class of materials manufactured from wood pulp or other natural sources of cellulose. During production the constituent cellulose polymer is dispersed into solution at the molecular level, either by temporary derivatisation, by complex formation or by direct dissolution [1,2]. The viscous polymer solution is then extruded through spinnerets and regenerated or precipitated into filaments, which are then washed, dried and further processed for different applications. The end uses of cellulosic fibres are many and varied, including applications in apparel or technical textiles, or non-woven textiles such as wipes and filters, or non-textile technical materials, including health-care and medical products.

Many aspects of the performance of cellulosic fibres are concerned with their response towards liquid or atmospheric water. Their mechanical properties are highly moisture sensitive, offering the opportunity to control modulus and yield response during processing, for example during ironing or pressing. The uptake of water vapour and liquid water by garments plays an important role in the experience of clothing comfort [3,4], which is associated with the transmission of perspiration away from the body. Comfort is also associated with the interaction of water with cellulose at the molecular level [5], which induces a strong exothermic sorption response, with an equivalent endothermic response induced as water is evaporated [6,7]. The nanoscale textures created in cellulosic fibres during regeneration have a high liquid holding capacity, as pore spaces are opened between cellulose polymer domains [8–10]. The rapid uptake of water into the fibre internal volume is ideal for technical applications where high absorbency is required [11]. In addition, the chemical processing of cellulosic fibres is often carried out by treatment in aqueous solutions, as in dyeing or cross-linking [12]. Agents are delivered into the expanded pore structure of the fibres, which then react at cellulose sites at the internal surfaces, forming physical or covalent bonds [13,14]. An understanding of the interaction of water with cellulose at the molecular level is therefore essential for the interpretation and prediction of fibre performance in use [5,15]. Such molecular interactions will depend on the structure and chemistry of the internal cellulose surfaces, which will be sensitive to the effects of different processing technologies [16,17].

NMR techniques are well-placed to provide information about water at the molecular level, as the resonance phenomenon is

* Corresponding author. Tel.: +44 (0)161 3063173; fax: +44 (0)161 3064153.
E-mail address: roger.ibbett@manchester.ac.uk (R.N. Ibbett).

0032-3861/$ – see front matter © 2008 Elsevier Ltd. All rights reserved.
doi:10.1016/j.polymer.2008.08.053

uniquely sensitive to both local chemical and dynamic effects. In addition, the selectivity of the technique means that it can be used to observe only species concerned with the relevant water environments, by selection through dynamic means or tuning to particular nuclei [18,19]. Cellulosic fibres are not amenable to conventional high-resolution solution NMR methods, as the chemical shift information is degraded by solid-state nuclear interactions and heterogeneities. However, carbon-13 solid-state magic angle spinning (MAS) techniques have been widely used for the study of cellulose supramolecular structure and by inference the interactions between the cellulose polymer phase and water [20,21]. Alternatively, low-resolution proton relaxation time techniques offer a direct method for studying water behaviour in cellulosic materials, applicable to any state of hydration from ambient to saturated and beyond. Early work by Carles and Scallan demonstrated that a simple two-site model could be used for the interpretation of T_2 (transverse) relaxation times in cellulosic materials, where water molecules were in fast diffusive exchange between interacting and non-interacting environments [22]. This model has been successfully applied for characterisation of natural [23] and chemically modified cellulose materials [24], with a single relaxation parameter defining all water–polymer interactions. A more comprehensive diffusion-relaxation model was developed by Brownstein and Tarr, which includes the effects of intermediate or slow diffusive exchange of water within hydrated void structures, leading to multi-exponential T_2 behaviour [25]. Later work by Hills on other biopolymers and synthetic analogues has shown that the essential interactions with water are influenced by both molecular diffusive and proton chemical exchange [26,27]. These studies made use of the earlier theory of Swift and Connick, which describes the NMR relaxation of water undergoing chemical exchange between different solution environments [28]. In a more recent variable temperature study, McConville and Pope considered that interactions between water and hydroxy functional polymer gels could be due to a combination of proton chemical exchange and restriction of water molecular tumbling, which in a fast diffusive regime would lead to a single averaged T_2 relaxation time [29]. Overall there is still uncertainty over the local mechanisms governing water T_2 relaxation in regenerated cellulose materials, without which it is impossible to select the most appropriate of the available theoretical models or to establish a realistic morphological framework for water–cellulose interactions. The current study represents a further investigation of this important topic, with the aim of exploring and contrasting the models described above as tools for characterisation of cellulosic materials. To this end water proton T_2 measurements have been carried out at variable moisture contents, at variable pH and temperatures, using lyocell regenerated fibre and also comparative regenerated and natural cellulose products. Selected measurements have also been carried out substituting water for deuterium oxide, in an attempt to elucidate relaxation mechanisms and the populations of protons involved in different interactions.

1.1. Models

A simple two-site model, as first explored for cellulose by Carles and Scallan [22], assumes fast interchange on the NMR experiment timescale between populations of water at cellulose pore surfaces (S) and free water within pore interiors ($N-S$), according to Eq. (1). The total gravimetric water content is N. The intrinsic T_2 relaxation times for the surface and interior environments are (T_s) and (T_f) respectively, which are assumed to be constant at all sample water contents. The interior pore water is assumed to have the properties of bulk water, with a T_2 relaxation time around 2–3 s. The average observed relaxation time (T_{obs}) is therefore a simple function of the proportions of the two populations and can be used as a measure of internal hydrated surface area. The interaction of water molecules with the cellulose surfaces reduces (T_s) by several orders of magnitude below (T_f), so an approximate Eq. (2) is sufficient for practical use. In the past a value for T_s has been determined by extrapolation to low water content [22], or by freezing of the interior water [23], or from molecular correlation time analysis [24].

$$\frac{N}{T_{obs}} = \frac{(N-S)}{T_f} + \frac{S}{T_s} \tag{1}$$

$$\frac{N}{T_{obs}} = \frac{S}{T_s} \tag{2}$$

A specific form of this site-averaging model is described for a hydrated polymer where interaction with water is by chemical proton exchange with polymer hydroxyl groups. This is accounted for by the theoretical treatment of Swift and Connick [28], which may be applicable to cellulose. If the hydroxyl groups at the inner pore surfaces of cellulose are assumed to have rigid character then their intrinsic ^{1}H-T_2 relaxation times will be of the order of a few microseconds. In this scenerio the water protons exchanging with these groups will loose their magnetisation completely within the NMR experiment timescale, due to the strength of the dipolar interactions with neighbouring polymer protons. This limiting case of the Swift–Connick model is set out in Eq. (3), where the observed water T_2 relaxation (T_{obs}) is dependent almost entirely on the rate constant for chemical exchange. This is similar to the original Carles–Scallan two-site model for hydrated cellulose, where N is the water content as defined before and E is the population of exchangeable hydroxyl protons. As before, the non-interacting water protons are assumed to have a relaxation time equivalent to bulk water (T_f). A further relaxation time is defined for the rigid cellulose polymer (T_e), with a single water-hydroxyl proton exchange rate constant defined as k. From this equation it follows that a faster exchange of protons leads directly to a faster loss of magnetisation and a shorter observed relaxation time.

$$\frac{(N+E)}{T_{obs}} = \frac{N}{T_f} + \frac{E}{[T_e + (1/k)]} \tag{3}$$

A further treatment applicable to hydroxyl functional polymers has been proposed by McConville and Pope [29], which combines the features of both the Swift–Connick and Carles–Scallan models. This is set out as Eq. (4), where a relaxation parameter (T_s) is reintroduced to describe an additional population of physically interacting water molecules (S), which is restricted by the rigid hydrated polymer molecules. The terms E and k are defined as before in the water-hydroxyl exchange term of the Swift–Connick model. This now represents a three-site model, with water in fast diffusive exchange on the NMR timescale between non-interacting, mobility-restricted and rigid polymer hydroxyl environments. The model has been successfully applied to explain the single observed relaxation time behaviour of highly cross-linked hydrogels and may have similar merit for application to hydrated cellulose.

$$\frac{(N+E)}{T_{obs}} = \frac{(N-S)}{T_f} + \frac{S}{T_s} + \frac{E}{[T_e + 1/k]} \tag{4}$$

2. Experimental

Samples of three types of regenerated cellulose fibres were available from Lenzing AG, Austria. The lyocell fibre type is made by direct dissolution from an organic solvent, with the samples used

in this work produced by the TENCEL® process, from the solvent *N*-methyl-morpholine-*N*-oxide. (Lyocell type fibres can be made from other solvents, e.g. ionic liquids.) Viscose and modal fibres are both made using the xanthate derivatisation route. All manufactured fibres examined in this study were of 1.3 dtex grade, applicable for general textile end-uses, provided without spin-finish (lubricant). A sample of cotton was also selected, of American Upland grade, which was given mild neutral pH washing to remove gross contamination. The wax cuticle of this fibre resulted in a slower uptake of water but did not influence the total water capacity. A selection of wood pulp and cotton linter samples were also studied, processed under conditions to give differences in water capacity (saturated water content).

Samples of fibres were dosed with controlled amounts of distilled water on a microbalance. Wetted samples were randomised by hand (using latex gloves to avoid grease pickup) and were then packed into 10 mm pre-weighed glass NMR tubes. Other samples were retained at natural (atmospheric) moisture regain, to provide data at low water content. Tubes were sealed and reweighed and then equilibrated at 22 °C overnight before measurements. Following measurement the tubes were opened and placed in a vacuum oven at 100 °C overnight, to allow the samples to dry fully. The tubes were removed from the oven, resealed to allow them to cool, and finally reweighed. Sample water contents were calculated by difference and expressed on a dry weight basis.

Further samples were prepared at their fully saturated liquor contents. Portions of the fibres or other cellulose materials were immersed in excess water or in different pH buffer solutions for 30 min, and then transferred onto wire mesh supports within open ended centrifuge tubes. The centrifuge tubes were spun at 1600 *g* for 5 min to remove liquor external to the cellulose material, following which the samples were quickly weighed and then sealed within pre-weighed NMR tubes for equilibration. After measurements the tubes and samples were dried in a vacuum oven as before, prior to reweighing for determination of liquor contents.

NMR measurements were carried out on a Bruker Avance Instrument at 300 MHz proton frequency, using 10 mm tubes, or a Resonance Instruments Maran system operating at 23 MHz proton frequency, using either 10 or 18 mm probes. Temperature control for both instruments was available to an accuracy of +/0.1 °C The multiple echo CPMG (Carr–Purcell–Mieboom–Gill) sequence was used for water proton T_2 (transverse) relaxation time measurements of saturated and intermediate samples (90x-tau-[180y-tau]n-acquire) [30] at 25 °C. Unless otherwise stated a 50 μs tau delay was used with a 3 s recycle delay. On the Maran instrument it was possible to collect intensity data points consecutively after each refocusing echo, in order to acquire a complete one-shot decay profile. On the Bruker instrument FIDs (free induction decays) were collected sequentially at incremented cycle numbers (*n*) and were transformed to extract peak intensities. A solid-echo experiment (90x-tau-90y-acquire) was carried on various wet and dry lyocell samples at 23 MHz, at 25 °C, with 1 μs dwell time, a tau inter-pulse delay of 20 μs, a 13 μs pulse recovery delay following the second pulse, and a 3 s recycle delay. Simple pulse-acquire FID measurements were also used to determine the proton T_2 relaxation times of water in lyocell fibre at low moisture content, which could be differentiated easily as a longer decay component compared to the solid. CPMG relaxation profiles were fitted to functions describing either single or double (parallel) exponential decays, using Resonance Instruments WinFit non-linear least-squares fitting software, following automatic input of estimates. FID data was processed and analysed using commercial spreadsheet software.

Additional variable temperature CPMG measurements were carried out on lyocell fibre at 23 MHz, on a pH 7 buffer saturated sample of lyocell fibre. Relaxation profiles were collected after sample temperature stabilisation at 15, 25, 35, 45, 55 and 65 °C. Checks were made to confirm that the sample water content and probe tuning remained constant for all measurements.

Further fibre, cotton and pulp samples each weighing approximately 0.5 g were packed carefully into pre-weighed 18 mm NMR tubes, positioned to ensure that all material would be held within the zone of the transmitter/receiver coil. This was to ensure that the NMR response would be proportional to the amount of sample present. Before measurement the tubes and samples were dried in a vacuum oven at 100 °C overnight, to remove all physically held water. The tubes were capped, cooled and reweighed as before, for determination of sample dry weight. Following this, 4 ml of high purity deuterium oxide were quickly pipetted into each tube, ensuring all liquor would be within the coil zone, and tubes were then recapped tightly and allowed to equilibrate for 2 h at 22 °C. FID measurements of the sealed tubes were collected at 25 °C, under quantitative conditions, using constant receiver gain and number of scans for all samples, with a recycle delay of 10 s to ensure full spin-lattice relaxation of HDO protons. The FIDs of selected dried samples were collected before addition of deuterium oxide, and also of a blank sample of 2 ml of deuterium oxide. In all quantitative studies the probe tuning was checked and adjusted at each measurement.

A selection of the samples equilibrated in deuterium oxide were prepared at saturated liquor content by centrifugation at 1600 *g*, which were then reweighed and repacked into NMR tubes for measurement of their residual proton T_2 relaxation times, using the CPMG experiment, at 25 °C. After measurement the samples were dried and reweighed to determine their liquor contents, as previously described. The same centrifuge preparations and CPMG measurements were also carried out on a set of lyocell fibre samples equilibrated in a range of liquors which had been formulated volumetrically from 100% D_2O/0% H_2O in increments down to 0% D_2O/100% H_2O.

3. Results and interpretation

3.1. Relaxation

Fig. 1 shows the ^{1}H-T_2 relaxation time data for lyocell fibre samples prepared at a range of water contents, measured at 23 MHz at 25 °C. Single exponential relaxation behaviour was observed below the fibre saturation point, from water within the fibre, which became multi-exponential above saturation. Two exponential components were the minimum required to successfully describe the data above saturation, as characterised by non-

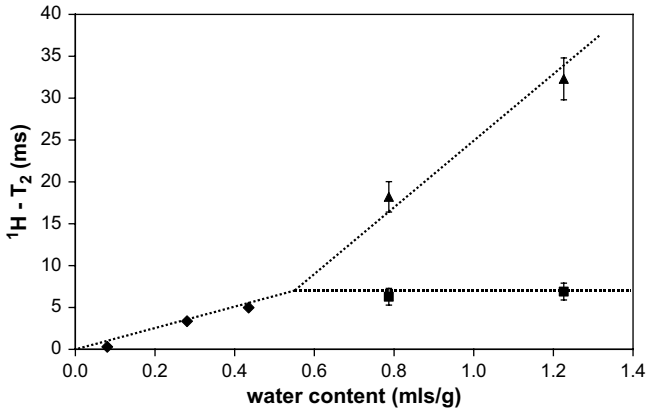

Fig. 1. Water ^{1}H-T_2 relaxation time analysis of lyocell fibre at different water contents, at 23 MHz, 25 °C: (◆) single exponential behaviour, (■, ▲) bi-exponential behaviour.

linear fitting, which indicated the presence of two separated water populations. The constancy of the relaxation time for the faster component above saturation suggested it was due to the internal water environment, with the slower component assigned to water external to the fibres. The proportion of the faster component varied slightly with total water content, indicating partial diffusive exchange with the external environments. Below saturation the single exponential T_2 values followed an approximately linear relationship with the fibre water content, which could be extrapolated successfully to zero intercept. This is consistent with the Carles–Scallan and Swift–Connick two-site average models, within the fast diffuse exchange regime, although these clearly break down as the new external water population develops [31,32]. Similar linear trends below saturation were found in this study for a range of both natural and regenerated materials. Typical data is shown for modal fibre in Fig. 2, at 300 MHz, which gave a best-fit linear extrapolation to the origin with $R^2 = 0.987$. From Fig. 1, the experimental water T_2 relaxation time becomes very short at low water contents, around the natural atmospheric regain [19]. In this regime the population of interior pore water does not exist and the two-site-averaging model is also inappropriate [33]. Atmospheric adsorbed water will be tightly physically constrained, with a short value for T_{obs} of around 300 μs seen for this sample at 8% moisture, as measured directly from the FID.

Systematic CPMG measurements were carried at 300 MHz at 25 °C, on a series of saturated lyocell fibre prepared following immersion in a range of pH buffer solutions. The gravimetric analysis confirmed that all samples had very similar liquor contents, so it could be assumed that the individual population weightings described in the site-averaged models would be constant. The graph in Fig. 3 reveals a striking reduction in the single exponential relaxation time (T_{obs}), at both low and high pH, which cannot be due to a change in total pore volume or to any alteration of the lyocell fibre morphology. Proton chemical exchange is known to be highly pH dependent and it is therefore most likely that this leads to the variations in relaxation behaviour, as elucidated by the theory of Swift and Connick. As discussed, one useful limiting condition of their model may be applicable to cellulose, set out in Eq. (3), where the exchangeable polymer groups have a very short T_2 relaxation due to the dominance of static nuclear dipolar interactions [27]. In order to test this assumption, the solid-echo relaxation profiles for lyocell fibre were measured at different moisture contents at 23 MHz, as shown in Fig. 4, where the rapidly decaying intensity from the cellulose polymer protons is distinct from the underlying response of water (extrapolated to back short times as dashed lines). The overlying

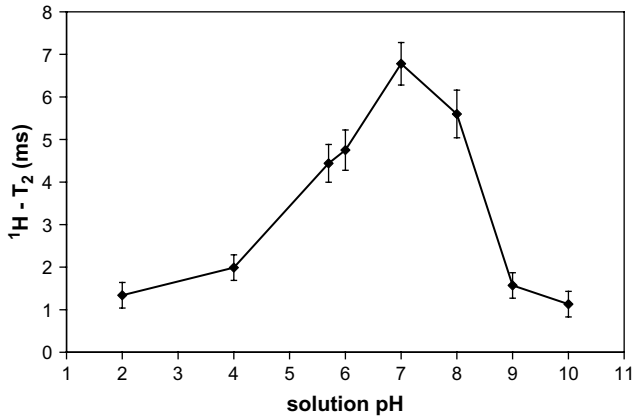

Fig. 3. variation in water ^{1}H-T_2 relaxation time of lyocell fibre, at 300 MHz, 25 °C, prepared at saturated liquor content from buffer solutions at differing pH.

fast polymer decay remains at constant magnitude for both dry (non-exchanging) and wet (exchanging) samples, so must account for both the carbon bonded protons and the hydroxyl protons of cellulose. The cellulose hydroxyl protons in their associated (bonded) state must therefore be considered as part of the solid, with their intrinsic T_2 relaxation defined by a Gaussian decay constant, which is typical for most rigid materials around 10–20 μs. As another test of the limiting assumption of the Swift–Connick model, the water T_2 relaxation times were measured over a wide range of CPMG inter-pulse (tau) spacings at 23 MHz and also at 300 MHz, at 25 °C, as plotted in Fig. 5. The lack of any dispersion, following the work of Hills et al. [27] is further a indication of the short relaxation time of the exchangeable polymer hydroxyl protons, causing them to loose magnetisation fully within the interval of the shortest tau time of 50 μs. In the absence of other relaxation mechanisms, the total observed relaxation time of water should therefore depend only on the rate of exchange between water and cellulose hydroxyl groups. However, as will be discussed, the differences in absolute ^{1}H-T_2 relaxation times between 23 and 300 MHz may be an indication that a motionally restricted environment of water does exist at cellulose surfaces, undergoing diffusional interchange with non-interacting environments within the tau period.

3.2. Chemical exchange

The usefulness of the Swift–Connick Eq. (3) for characterising hydrated cellulose can be further investigated by considering

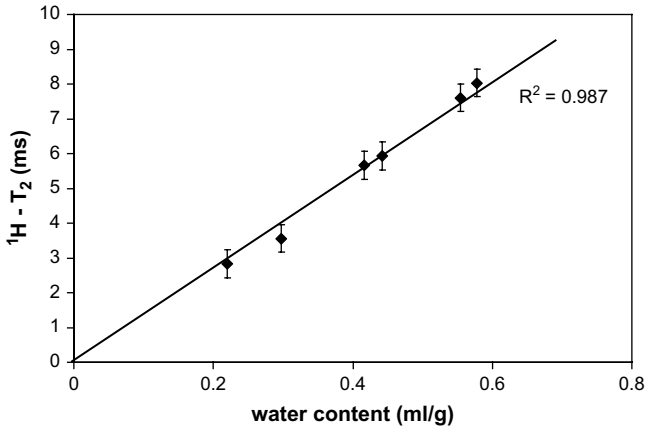

Fig. 2. Water ^{1}H-T_2 relaxation time analysis of modal fibre at different water contents below saturation, at 300 MHz, 25 °C. Linear best fit is shown extrapolated to zero intercept ($R^2 = 0.987$).

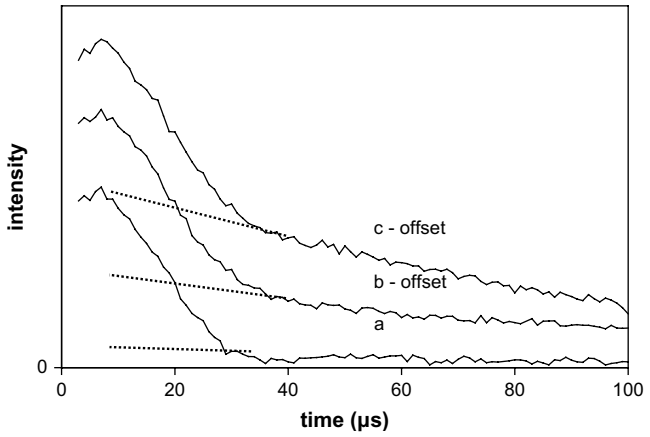

Fig. 4. Solid-echo ^{1}H free induction decay profiles of lyocell fibre at different water contents. (a) Oven dried, (b) approximately 20% water, (c) approximately 60% water.

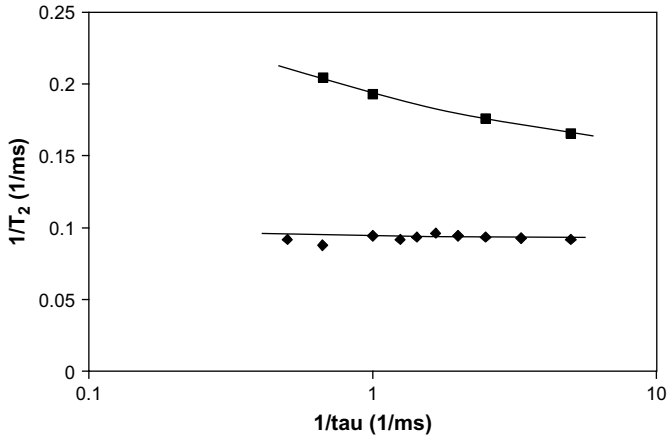

Fig. 5. Dependence of water ^{1}H-T_2 relaxation time in saturated lyocell fibre with CPMG inter-pulse (tau) spacing, at 25 °C, (◆) at 23 MHz, and (■) 300 MHz.

significance of the parameters for the proton exchange rate constant (k) and also the population of exchanging protons (E). In principle this second parameter can be found directly from a classical deuterium oxide exchange experiment, which in the past has been used to provide information about cellulose crystallinity and accessibility [34]. The FID of a fully dried cellulose sample exhibits no slow decay from adsorbed water, as shown in Fig. 6, at 23 MHz, with all cellulose hydroxyl protons contributing to the fast solid decay. The introduction of a large excess of deuterium oxide will liberate the accessible hydroxyl protons from the cellulose by chemical exchange, which will partition predominantly in the liquid and so be observed as a separate slow decay. From an attempted Gaussian fitting in Fig. 6 it is seen that the total intensity at zero time is apparently unchanged and that protons have merely been exchanged from solid to mobile environments. The classical cellulose accessibility (α) can be calculated from the magnitude of the slower decay using Eq. (5) and the moles of exchanging protons can be expressed on a water basis from Eq. (6) (where 2 mol of protons = 1 mol of water). This is referred to as E' to denote its independent determination. The moles of observed mobile protons (L) were determined in this work by simple extrapolation to the intensity axis, with reference to a pure water calibration sample. The total moles of cellulose hydroxyl groups (W) are known from the dry sample weight, where (D) is the total number of moles of deuterons added to the sample. The accessibilities determined in this way for the different cellulose samples are summarised in Table 1.

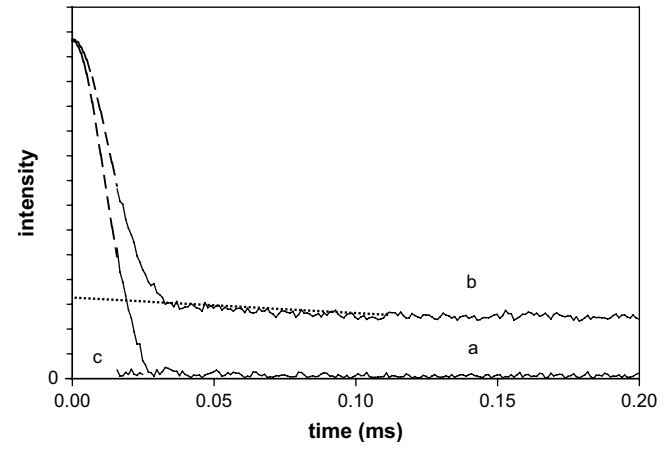

Fig. 6. ^{1}H FID decay of (a) oven dried lyocell and (b) same sample saturated with D_2O. Linear extrapolation of slow decay gives intensity of visible exchanging hydroxyl protons, with (c) intensity level for blank D_2O sample.

$$\alpha = \frac{LD}{W(D-L)} \tag{5}$$

$$E' = \frac{\alpha W}{2} \tag{6}$$

With an independently derived value for E', it is possible to rework Eq. (3) to calculate the water-hydroxyl exchange rate constant (k) from the T_{obs} relaxation times. This assumes that the cellulose accessibility is independent of pH, which should be valid provided that extreme conditions are avoided where cellulose degradation or swelling occurs. With E' for lyocell taken as 0.116 g/g from Table 1, the calculated exchange rate constants for the saturated fibre in the different pH buffer solutions are plotted as data points in Fig. 7. As expected the rate shows a distinct minimum under neutral conditions, rising at both low and high pH. Furthermore, from studies of proteins [35–37] and polysaccharides [38] it is known that mechanisms exist for both acid and base catalysed proton chemical exchange, according to the equilibria in Eqs. (7)–(9)

$$\mathrm{Cell{-}OH} + {}^{*}\mathrm{HOH} \underset{k_{-1}}{\overset{k_1}{\rightleftharpoons}} \mathrm{Cell{-}OH^{*}} + \mathrm{HOH} \tag{7}$$

$$\mathrm{Cell{-}OH} + \mathrm{H_3O^+} \underset{k_{-2}}{\overset{k_2}{\rightleftharpoons}} \mathrm{Cell{-}OH_2^+} + \mathrm{H_2O} \tag{8}$$

$$\mathrm{Cell{-}OH} + \mathrm{OH^-} \underset{k_{-3}}{\overset{k_3}{\rightleftharpoons}} \mathrm{Cell{-}O^-} + \mathrm{H_2O} \tag{9}$$

$$\upsilon = k_1[\mathrm{H_2O}][\mathrm{cell{-}OH}] + k_2[\mathrm{H_3O^+}][\mathrm{cell{-}OH}] + k_3[\mathrm{OH^-}][\mathrm{cell{-}OH}] \tag{10}$$

$$k = k_1[\mathrm{H_2O}] + k_2[\mathrm{H_3O^+}] + k_3[\mathrm{OH^-}] \tag{11}$$

The rate constants for the forward and backward catalysis reactions have fixed proportionality, resulting from their linkage via the reaction equilibrium constant (e.g. $K_1 = k_1/k_{-1}$). If the rate of each reaction is proportional to its forward rate constant multiplied by the reactant concentrations, then the combined rate (υ) for all three reactions is given by Eq. (10). The total first-order rate constant for proton exchange (k) is defined with respect to cellulose reactant concentration, which is then related to the acid, base and water concentrations by Eq. (11). All relevant concentrations can be calculated from the pH value, so this equation can be used to fit the experimental exchange rate constants determined from the T_{obs} data. For the buffered lyocell samples the most successful fit is shown in Fig. 7, with $k_1 = 2.1 \times 10^1\ s^{-1}$, $k_2 = 1.0 \times 10^6\ s^{-1}$ and $k_3 = 2.0 \times 10^8\ s^{-1}$ at 25 °C. Similar fitted curves with values of $k_1 = 1.4 \times 10^3\ s^{-1}$, $k_2 = 3 \times 10^7\ s^{-1}$ and $k_3 = 6 \times 10^9\ s^{-1}$ have been established for glucose in water from dispersion analysis [38], with $k_1 = 1\text{–}5 \times 10^2\ s^{-1}$ for synthetic hydrogels at 28 °C [29]. No doubt the lower values found in the current study can be ascribed to the lower degree of freedom at the cellulose–water interface compared to the solution or gel state. Use of the Swift–Connick model for prediction of pH dependent kinetics is further evidence of the importance of chemical exchange in explaining water proton T_2

Table 1
Water ^{1}H-T_2 relaxation data at 300 MHz, 25 °C, and corresponding deuterium exchange data for regenerated fibre and pulp materials

Sample	N (ml/g) water saturation capacity (SD = 0.01)	α Deuterium oxide accessibility (SD = 0.015)	E' (ml/g) total deuterium-exchanging water	T_{exp} (ms) (300 MHz) (sat pH 7) (25 °C) (SD = 0.05)	E (ml/g) $k = 1.24$ ms^{-1}; $T_e = 18$ μs surface exchanging water (Eq. (3))	f correction factor for k	S (Eq. (4), using E') (ml/g) $k = 0.81$ ms^{-1}; $T_e = 18$ ms; $T_s = 2.38$ ms surface interacting water	S (Eq. (1)) (ml/g) $T_s = 0.96$ ms surface interacting water	d ($d = 0.57/f$) (nm) cellulose accessible layer thickness
Lyocell	0.69	0.70	0.116	5.5	0.116	1.00	0.116	0.116	0.57
Viscose	0.90	0.80	0.132	9.0	0.090	0.72	0.020	0.096	0.79
Modal	0.62	0.74	0.122	5.8	0.102	0.86	0.066	0.102	0.66
Cotton	0.44	0.43	0.070	5.9	0.071	1.00	0.066	0.072	0.57
Paper pulp	0.88	0.68	0.113	9.4	0.084	0.77	0.033	0.090	0.74
Dissolving pulp (1)	0.68	0.57	0.094	6.9	0.092	0.98	0.080	0.095	0.58
Dissolving pulp (2)	0.68	0.60	0.099	7.2	0.088	0.89	0.063	0.091	0.64
Cotton linters (1)	0.47	0.47	0.078	5.9	0.076	0.98	0.066	0.076	0.63
Cotton linters (2)	0.52	0.43	0.071	6.7	0.073	1.02	0.068	0.075	0.57

relaxation in cellulose. The fit in Fig. 9 is quite respectable apart from an apparent underestimation of exchange rate at high and low pH limits, which may be evidence of a diffusion limit in exchange rate regardless of the effectiveness of acid or base catalysis.

The applicability of an independently determined value for E' in the Swift–Connick model can be investigated if the total water–cellulose proton exchange rate constant (k) is considered to be invariant. This would be the case at controlled (neutral) pH and temperature, meaning that the entire exchange related term in Eq. (3) should therefore also be constant [$T_e + 1/k$]. It could then be argued that this term should be a constant for any saturated cellulose material, so Eq. (3) can then be used to back-calculate a value for (E) simply from a determination of the T_{obs} relaxation time and the total water content (N). A value for k of 1.24 ms^{-1} is taken from the fitted lyocell data at pH 7, at 300 MHz, in Fig. 7, and $T_e = 0.018$ ms for the solid cellulose relaxation time, which of course returns a value of 0.116 ml/g for lyocell by this circular argument. However, once k and T_e are standardised this procedure will provide meaningful comparative values for E for the other cellulose materials (without subscript to denote its determination from relaxation data). Any deviations between E' and E may point to an oversimplification of the Swift–Connick model but more importantly may provide additional morphological information concerning the cellulose hydrated state. Indeed, although this comparison in Fig. 8 does suggests a loose agreement between (E) and (E') for the different classes of cellulose materials, the poor correlation seen for the regenerated fibres suggests that there may be non-exchange contributions to T_2 relaxation, or else the effective proton exchange rate (k) varies between different morphologies.

3.3. Exchange and mobility

The presence of non-exchange contributions to T_{obs} in cellulosic materials can be investigated by the substitution of proteo- for deutero-water, in order to separate inter-molecular from intra-molecular relaxation mechanisms [39,40]. Firstly, the proton T_2 relaxation times of residual HDO protons in the D_2O saturated cellulose fibres are compared with the equivalent data for relaxation in H_2O, at 23 MHz at 25 °C, in Table 2. Deuterium is very much less efficient as a source of relaxation than hydrogen [40], so the absence of protons in the water phase of these samples might be expected to lead to a severe lengthening of the measured T_2 times, resulting from the lack of proton-proton intra-molecular interactions. However, the results in Table 2 show that relaxation is still highly efficient, which is confirmation of a strong inter-molecular interaction between the water protons and the cellulose internal surfaces. The ranking between the fibres remains very similar to that in H_2O, which is further evidence that inter-molecular relaxation is influenced by fibre morphological factors.

Proton chemical exchange must contribute significantly to the inter-molecular surface relaxation mechanism, but this could also be supplemented by a further physical contribution simply due to motional restrictions at the interface, which would also result in inter-molecular relaxation through static dipolar interaction with

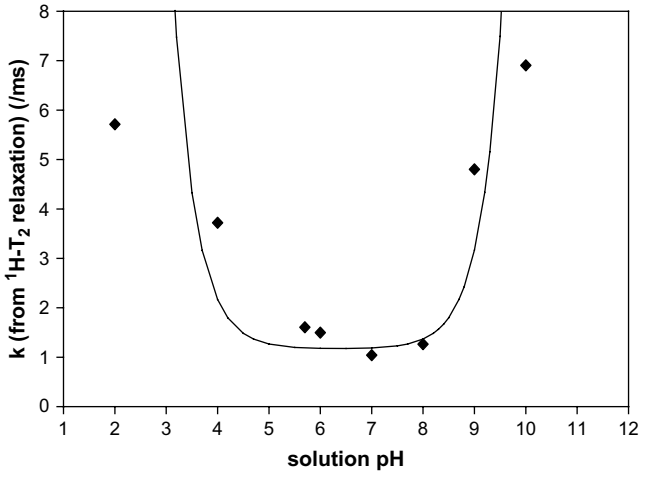

Fig. 7. Exchange rate constants (k) at 25 °C, derived from water ^{1}H-T_2 relaxation times in saturated lyocell fibre, (◆) using Eq. (3). Continuous line is fit to Eq. (10) with $k_1 = 2.1 \times 10^1$ s^{-1}, $k_2 = 1.0 \times 10^6$ s^{-1} and $k_3 = 2.0 \times 10^8$ s^{-1}.

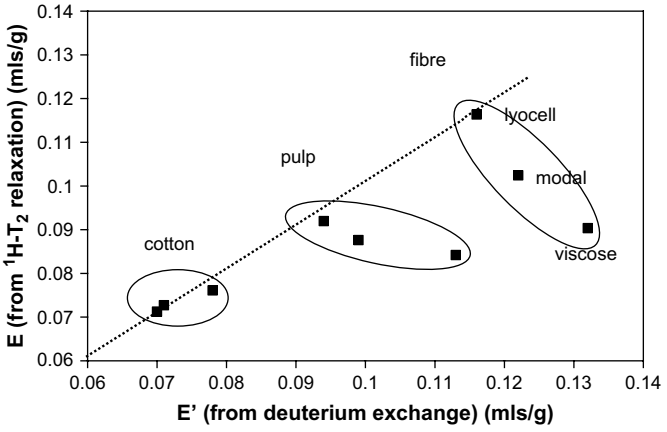

Fig. 8. Comparison of amount of exchanging protons in cottons, pulps and regenerated fibres (expressed on a water basis) determined either by ^{1}H-T_2 relaxation (E), or by deuterium exchange (E'). Dashed line is 1:1 correspondence.

Table 2
^{1}H-T_2 CPMG relaxation data at 23 MHz, 25 °C for different regenerated fibres

Fibre	H_2O-T_2 (ms) (23 MHz) (sat pH 7) (25 °C) (SD = 0.05)	N (ml/g) (for 23 MHz data) (SD = 0.01)	HDO-T_2 (ms) (in unbuffered D_2O) (SD = 0.1)	S (ml/g) Eq. (1) T_s = 1.24 ms
Lyocell	7.6	0.71	35	0.116
Viscose	12.3	0.92	45	0.093
Modal	7.2	0.60	30	0.103
Cotton	8.9	0.41	29	0.057

cellulose protons [41]. In addition, a separate intra-molecular dipolar relaxation pathway might also be possible for water at cellulose surfaces, due to static dipolar interaction between proton pairs on the same molecule. However, this would be effective only in proteo-water and not for the residual unpaired protons of deutero-water. Thus it can be argued that proton relaxation in H_2O might be enhanced by a contribution that is absent from that in residual HDO, so the differing relaxation behaviour in H_2O and D_2O offers some means by which motional restriction and exchange effects can be separated. The data in Fig. 9, at 23 MHz, shows how the proton relaxation rate ($r_{obs} = 1/T_{obs}$) for saturated lyocell is dependent on the extent of deuteration, which should follow a relationship governed by the balance of relaxation contributions. Firstly, it is assumed that water relaxation away from the cellulose surface is of negligible significance. Then it can be assumed that a purely intra-molecular contribution to the relaxation rate will follow the probability of proton pairing on the same water molecule, calculated from the extent of deuteration. As shown in Fig. 9, this will tend in a non-linear manner to a very low value as the chance of finding two protons on a water molecule approaches zero. On the other hand, a purely inter-molecular contribution to the relaxation rate will follow a simple linear probabilistic relationship as 3 in 10 of the protons on a cellulose unit are progressively substituted for deuterons, also as shown in Fig. 9. Most importantly, this second relationship would apply to both motional restriction or exchange contributions, as in either case the substitution of protons for deuterons would reduce the effective dipolar relaxation strength of the cellulose interface. This would apply regardless of whether the protons were simply in close proximity to the cellulose polymer or were actually exchanged onto hydroxyl groups. The observed relaxation rate (r_{obs}) follows neither of these predicted relationships instead taking an intermediate path. This is strong indication that both intra-molecular (motional) and inter-molecular (motional or exchange) mechanisms are active, so

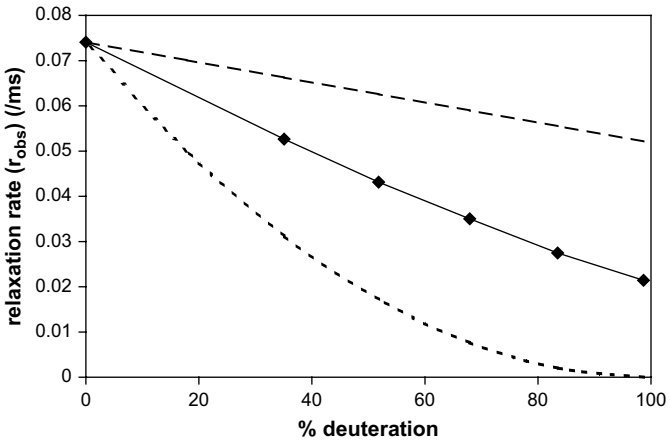

Fig. 9. Water ^{1}H-T_2 relaxation rate (r_{obs}) for lyocell fibre saturated at different D_2O/H_2O ratios. (◆) Experimental data, (—) prediction for intra-molecular mechanism only (motional), (– – –) prediction for inter-molecular mechanism only (motional or exchange).

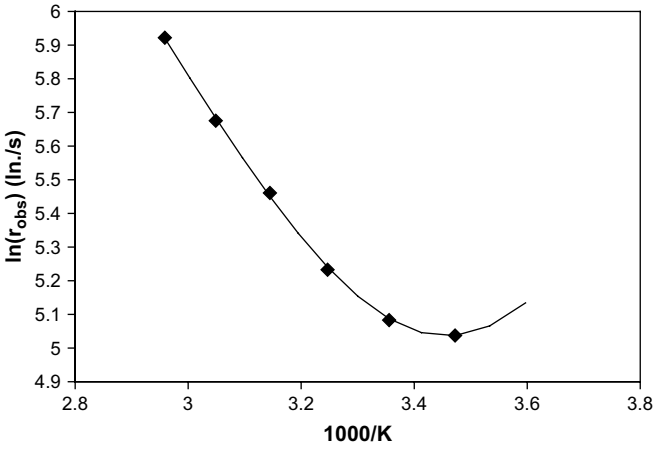

Fig. 10. Arrhenius plot in the temperature range of 15–65 °C for relaxation rate (R_2) of pH 7 buffer saturated lyocell. (◆) Experimental relaxation data, (line) fit using proton exchange rate and water correlation time from McConville–Pope model.

indeed a separate population of motionally restricted water can be invoked to fully describe relaxation behaviour.

The viscosity of D_2O is around 25% greater than H_2O and will have an influence on relaxation as the liquid composition is changed. The experimental relaxation rates in Fig. 9 have been corrected accordingly, with the values reduced in line with the fraction of deuterons present, up to a maximum of 25% in the fully D_2O substituted liquor. Also, deuterium chemical exchange rates are slower than proton exchange rates, referred to as a primary isotope effect [38]. However, since we are considering only proton behaviour it could be argued that this additional influence on the exchange contribution to relaxation can be ignored.

The composite model set out by McConville and Pope may provide a more complete description of water relaxation in cellulosic materials, where contributions are included from both proton exchange and from motional restriction [29]. Their methodology is underpinned by measurements of T_{obs} at a range of temperatures, followed by Arrhenius analysis, which is a technique that can also be applied to samples of hydrated cellulose [42]. Water T_2 measurements were carried out on lyocell fibre saturated at pH 7, at 23 MHz, spanning an accessible range of temperatures (15–65 °C), in order to generate an Arrhenius plot based on the generic Eq. (12). As usual, r is a rate constant (in this case the observed relaxation rate, $r_{obs} = 1/T_{obs}$), B is a thermal activation energy in kJ/mol, R is the gas constant, T is the temperature in Kelvin units and A is an Arrhenius pre-exponential parameter. This plot, in Fig. 10, shows marked curvature, providing evidence of two thermally activated processes, for the separate proton exchange and water mobility contributions to relaxation

$$r = Ae^{-B/RT} \tag{12}$$

$$r_C = \frac{Q}{3}\left[3\tau_C + \frac{5\tau_C}{1+\omega_o^2\tau_C^2} + \frac{2\tau_C}{1+4\omega_o^2\tau_C^2}\right] \tag{13}$$

A fitting exercise was carried out on the lyocell relaxation data, using Eq. (4), with the aid of Microsoft Excel Solver™, to establish the Arrhenius parameters for water–cellulose exchange (B_{ex}, A_{ex}) and water mobility (B_s, A_s). In Eq. (4) the extent of motional restriction of water is accounted for by the relaxation parameter (T_s) which is itself assumed to be dependent on a single water rotational correlation time (τ_s), according to the BPP theory of

relaxation [29], from Eq. (13). Here Q is a constant appropriate for water intra-molecular dipolar relaxation ($Q = 5.33 \times 10^9\ s^{-2}$), and ω_0 is the spectrometer frequency. Actually it is the correlation time (τ_s) for water tumbling which has Arrhenius temperature dependent behaviour, which exerts a corresponding influence on the NMR relaxation rate. Fitting was simplified by eliminating the bulk water term (T_f) and by using the independently determined values for N and E'. As can be seen from Fig. 10, the curvature of the experimental data can be modelled successfully, with the model parameters summarised in Table 3.

However, as might be anticipated from the Pope–McConville Eq. (4) it is not possible to separate the T_s and S parameters in the fitting exercise, as it is their ratio which influences the magnitude of the water motional contribution to relaxation. The knowledge of the ratio does at least allow an independent estimation of the weighting of the total contribution due to motional restriction of water, which is around 30% of the total relaxation rate over a wide range of values of S. This implies a reduction in the chemical exchange rate constant (k) predicted from the data in Fig. 7, from 1.24 ms^{-1} at 300 MHz, 25 °C and pH 7, without the mobility contribution, to 0.81 ms^{-1} with its inclusion. This purely physical contribution might be lower than that suggested from the deuteration data in Fig. 9, where the experimental data points are roughly halfway between the two predicted lines. Previous workers have suggested a cyclic mechanism for exchange under neutral conditions [38], which would involve both deuterons and protons in a partially deuterated liquor. The rate of proton exchange detected by NMR might therefore be retarded by the heavier deuterons at other positions around the cycle.

4. Discussion

An objective for the current work was to provide interpretational tools to account for the morphological influences on the water relaxation in cellulose. One approach might therefore be to fix a value for the surface relaxation parameter (T_s), and to use the McConville–Pope Eq. (4) with the aid of the separately determined E' and (N) to calculate a value for S. This term (S) would act as a measure of the population of motionally interacting water at cellulose interfaces, relating to inner surface area. Using lyocell as a reference, the required constant for the surface relaxation parameter (T_s) could be established by setting $E' = S = 0.116$ ml/g, which may be physically valid if the cellulose interface for lyocell consists of only a single cellulose layer [43]. This makes the argument that every accessible glucan unit will contribute three protons or 1.5 water molecules by chemical exchange, so these protons will be manifested in their water associated state as the physically interacting water population (S). This leads to value for T_s of 2.38 ms at 25 °C from Eq. (4), at 300 MHz, which implies that the physical restriction of the interfacial water is quite weak. Other workers have suggested that the interactions in proteins may be much stronger but involving many fewer water molecules, which may relate to specific binding centres [39,40]. The concept of chemical or stereochemical binding is not however felt to be appropriate to cellulose where the internal interface will most likely consist of an array of hydroxyl groups all in very similar environments [20]. The values for S for the other cellulosic materials are summarised in Table 1, calculated from Eq. (4) for the 300 MHz data, with $T_s = 2.38$ ms, $T_e = 18$ μs, and $k = 0.81\ ms^{-1}$, at 25 °C and pH 7.

The equivalence between the population of surface interacting water molecules (S) and exchangeable hydroxyl protons (E') may be reasonable for lyocell, where it is believed that the accessible hydroxyl groups are concentrated at the immediate cellulose–water interface [20]. However, a high value for E' means that relaxation predicted by the McConville–Pope Eq. (4) is biased in favour of the exchange contribution, which therefore becomes dominant over the contribution from motional restriction. According to the data in Table 1 this leads to unacceptably low values for S for the samples with high deuterium oxide accessibility such as viscose fibre and the paper pulp. From other techniques these materials are known to have high internal surface areas [14], suggesting a large population of surface interacting water.

The alternative Swift–Connick Eq. (4) can be used to gain useful morphological insights by considering the reduction in the effective exchange rate constant (k) required to bring the value of E into line with the separately determined value for E' from deuterium exchange. This reduction would be valid if the accessible cellulose were organised as a thicker accessible interface, or indeed in separate accessible polymer domains, so hydroxyl groups beneath the immediate interface had slower exchange rates with water. These reduction factors (f), in Table 1, do appear to follow anticipated structural differences between the various materials, with the cotton fibres and linter samples, along with lyocell, requiring the least correction. As discussed, the accessible fraction in lyocell and also cotton is considered to exist as a single molecular layer [34]. In comparison, viscose may contain accessible polymer in a fringe-micelle morphology, and in the case of the paper pulp a proportion of the hydroxyl accessibility may be due to its high hemicellulose content (around 18% by weight) The dissolving pulps represent an intermediate case where refinement has removed some accessible disordered polymer, either through extraction of hemicellulose or recrystallisation. From simple diffusion arguments, the exchange rate reduction factor (f) may be considered to be inversely proportional to the thickness of the accessible polymer region at the interface, where the value of $f = 1$ represents a single polymer chain thickness, which is around 0.57 nm [44]. The apparent thicknesses of the exchangeable cellulose component then follow from this reference dimension, also listed in Table 1.

The suggestion that buried hydroxyl groups have lower exchange rates implies that only the fastest proton exchange at the immediate interface contributes to NMR T_2 relaxation. This can be illustrated in Fig. 11, where the internal exchange rate between water and hydroxyl groups (k_i) is lower than the interfacial rate (k_s). In this case water proton T_2 relaxation will be sensitive only to direct surface contact with the cellulose phase, regardless of the total cellulose exchange capacity. Under conditions of strictly controlled pH this justifies the use of the original Carles–Scallan two-site Eq. (1), which requires no definition of the relaxation mechanism at the cellulose surface. A value of $S = 0.116$ ml/g for lyocell is applied again for standardisation, in order to derive a surface relaxation parameter $T_s = 0.96$ ms, which should be usable for the other cellulosic materials, at pH 7, at 25 °C, at 300 MHz, with values for S listed in Table 1.

The removal of the strict linkage between T_2 relaxation and deuterium exchange means that the respective parameters (S) and (E') can be considered as separate indicators of the material morphology. The meaning of E' is simply a measure of equilibrium cellulose accessibility, and should correlate inversely with crystallinity and crystallite size [34]. As already suggested, the S parameter in the Carles–Scallan model should correspond to the immediate

Table 3
Arrhenius parameters from variable temperature CPMG ^{1}H-T_2 measurements of pH 7 buffer saturated lyocell at 23 MHz

	Eq. (4)
B_{ex} (kJ/mol)	10.9
B_c (kJ/mol)	13.0
A_{ex} (s^{-1})	1.9×10^7
A_c (s^{-1})	3.5×10^{13}

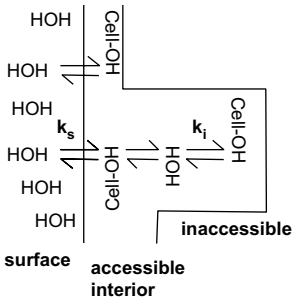

Fig. 11. Schematic showing proton exchange between water in pores and accessible cellulose hydroxyl groups. Rate constants k_s for faster immediate exchange into water phase and k_i for slower exchange within thicker accessible region.

surface area of the internal pores undergoing interaction with water and therefore should correlate inversely with average pore size.

The determination of surface interacting water (S) from the Carles–Scallan Eq. (1) suggests a lower surface area for the cotton samples, and higher values for the pulps. The hemicellulose of the paper pulp should only act by way of its immediate water interface, so the S value should still be representative of the internal pore area. The regenerated fibres have even higher amounts of surface acting water, with lyocell the highest of all. Viscose still has a lower value for S than the other fibres, despite its high total saturation capacity, which is in contrast with data from size exclusion measurements [14]. However, it must be remembered that ^{1}H-T_2 relaxation is directly responsive to the extent of water–cellulose interfacial contact, whereas for size exclusion measurements the surface area is calculated indirectly from pore volume, and may therefore suffer from deviations caused by bottle-neck effects. Such pore entry restrictions could result in a higher calculated surface area for viscose, which has a less oriented pore structure than lyocell [45]. The ranking of the regenerated fibres remains similar when measurements are carried out at the lower field strength of 23 MHz although this requires a different value for T_s of 1.24 ms under the same pH buffer and temperature conditions. As described earlier, from Fig. 5, the field strength dependence of ^{1}H-T_2 relaxation is a further complexity, as there is no obvious dispersion in the CPMG experiment. However, we have identified the existence of a population of water experiencing physical interaction with cellulose, which may exhibit a chemical shift difference from non-interacting water via chemical or magnetic susceptibility effects. This water apparently experiences only a moderate increase in dipolar relaxation strength so will retain partial magnetisation within the tau period. Diffusive interchange with non-interacting water within the tau time will lead to a contribution to relaxation through dephasing, which will become much more significant at the much higher 300 MHz field strength. From Fig. 5, the increase in water T_2 relaxation time with decreasing tau at 300 MHz is also consistent with the existence of a diffusional interchange mechanism [27].

The McConville–Pope Eq. (4) may offer the best interpretation of water behaviour in hydrated cellulosic fibres, which in principle can account for morphological factors influencing both proton chemical exchange and physical interactions of water at cellulose internal surfaces. However, variable temperature experiments may be necessary to attempt a separation of the different variable parameters, which may not be achieved fully without the use of more sophisticated methodologies. This fruitful area of study will be pursued further.

5. Conclusions

This work has shown that two-site models can be suitable for the interpretation of proton T_2 relaxation behaviour of water in regenerated cellulosic fibres, provided that measurements are carried out constant neutral pH. Single exponential relaxation times are observed below the fibre saturation limit as water interchanges rapidly on the NMR timescale between all separate magnetic environments. Experiments at variable pH and variable temperatures have shown that the shortened relaxation times of water within saturated fibres are due largely to proton chemical exchange with accessible cellulose hydroxyl groups at pore surfaces. Proton exchange is accelerated by both base and acid catalyses and relaxation data has been used to estimate the rate constants for acid, base and neutral exchange mechanisms. Comparisons using the deuterium oxide exchange technique have shown that accessible regions beneath the immediate water–cellulose internal interfaces may not contribute effectively to the proton exchange relaxation mechanism. The amount of surface interacting water determined from NMR data is therefore sensitive only to the direct pore surface area. Differences between cellulose interacting water from T_2 relaxation and from deuterium exchange can therefore provide an estimate of the apparent depth of the accessible interfacial layer. These layer dimensions are greater for viscose and modal regenerated fibres than for lyocell. NMR relaxation also suggests that lyocell has a higher pore surface area than viscose or modal fibres, despite its higher crystallinity compared to the other fibres. This work has also shown that water interacting with the pore surfaces of hydrated cellulose materials experiences a restriction of mobility, allowing an intra-molecular dipolar contribution to relaxation, which can be accounted for using an extended three-site model. All site-averaged models are effective in the saturated fibre state as individual water molecules are diffusing very quickly between all internal fibre environments and there is no suggestion of long-lived binding interactions to specific cellulose sites.

Acknowledgement

This work was carried out with financial support from the Christian Doppler Research Society, Vienna, Austria.

References

[1] Moncrief RW. Man-made fibres. 5th ed. London: Haywood Books; 1970.
[2] Fink H-P, Weigel P, Purs HJ, Ganster J. Progress in Polymer Science 2001;26:1473.
[3] Umbach KU. Melliand Textilberichte 1981;3:360.
[4] Li Y. The science of clothing comfort. Nos. 1–2. In: Textile progress, vol. 31. Manchester, UK: The Textile Institute; 2001 [chapters 5 and 6].
[5] Schuster KC, Suchomel F, Männer J, Abu-Rous M, Firgo H. Macromolecular Symposium 2006;244:149.
[6] Kawai T. Journal of Polymer Science 1959;37:181.
[7] Bertran MS, Dale BE. Journal of Applied Polymer Science 1986;32:4241.
[8] Laity PR, Glover PM, Godward J, McDonald PJ, Nay JN. Cellulose 2000;7:227.
[9] Cameron RE, Crawshaw J. Polymer 2000;41:4691.
[10] Abu Rous M, Ingolic E, Schuster KC. Cellulose 2006;13:411.
[11] Bredereck K. Review of Progress of Coloration 2005;35:39.
[12] Bredereck K, Saafan A. Die Angewandte Makromolekulare Chemie 1981;95:13.
[13] Ibbett RN, Phillips DA, Kaenthong S. Dyes and Pigments 2006;71:168.
[14] Ibbett RN, Phillips DAS, Kaenthong S. Journal of Materials Science 2007;42:6809.
[15] Czihak C, Müller Schober H, Heux L, Vogel G. Physica B 1999;266:87.
[16] Maloney TC, Johansson Tuija, Paulapuro H. Paper Technology 1988;July:39.
[17] Ibbett RN, Phillips DAS, Kaenthong S. Dyes and Pigments 2007;75:624.
[18] Häggkvist M, Li T-Q, Ödberg L. Cellulose 1998;5:33.
[19] Child TF. Polymer 1972;13:259.
[20] Ibbett RN, Domvoglou D, Fasching M. Polymer 2007;48:1287.
[21] Newman RH, Davidson TC. Cellulose 2004;11:23.
[22] Carles JE, Scallan AM. Journal of Applied Polymer Science 1972;17:1855.
[23] Ono H, Yamada H, Matsuda S, Kunihiko O, Kawamoto T, Iijima H. Cellulose 1998;5:231.
[24] Baumgartner S, Lahajnar G, Sepe A, Kristl J. AAPS PharmSciTech 2002;3(4). article 36.
[25] Brownstein KR, Tarr CE. Physical Review A 1979;19:2446.
[26] Belton PS, Hills BP, Raimbaud ER. Molecular Physics 1988;63:825.
[27] Hills BP, Wright KM, Belton PS. Molecular Physics 1989;67:1309.
[28] Swift TJ, Connick RE. Journal of Chemical Physics 1962;37:307.
[29] McConville PM, Pope JM. Polymer 2001;42:3559.

[30] Harris RK. Nuclear magnetic resonance spectroscopy: a physicochemical. Longman Scientific and Technical; 1986 [chapter 3].
[31] Araujo CD, MacKay AL, Whittall KP, Hailey JRT. Journal of Magnetic Resonance Series B 1993;101:248.
[32] Topgaard D, Söderman O. Cellulose 2002;9:2002.
[33] Froix MF, Nelson R. Macromolecules 1975;8:726.
[34] Ioelovitch M, Gordeev M. Acta Polymerica 1994;45:121.
[35] Hills BP, Takacs Belton PS. Molecular Physics 1989;67:919.
[36] Rhol CA, Baldwin RL. Biochemistry 1994;33:7760.
[37] Woodward CK, Hilton B. Biophysics Journal 1980;10:561.
[38] Hills BP. Molecular Physics 1991;72:1099.
[39] Eisenstadt M. Biochemistry 1985;24:3407.
[40] Kiihne S, Bryant RG. Biophysical Journal 2000;78:2169.
[41] Garvey CJ, Parker IH, Simon P, Whittaker AK. Holzforschung 2006;60:409.
[42] Banas K, Blicharska B, Dietrich W, Kluza M. Holzforschung 2000;54:501.
[43] Ibbett RN, Domvoglou D, Phillips DAS. Cellulose 2008;15:241.
[44] Newman RH. Solid State Nuclear Magnetic Resonance 1999;15:21.
[45] Lenz J, Schurz J, Wrentschur E. Colloid and Polymer Science 1993;271:460.